Spatially resolved, single-ended two-dimensional visualization of gas flow phenomena using structured illumination

Kristensson, Elias; Richter, Mattias; Pettersson, Sven-Göran; Aldén, Marcus; Andersson-Engels, Stefan

Published in:
Applied Optics

DOI:
10.1364/AO.47.003927

2008

Spatially resolved, single-ended two-dimensional visualization of gas flow phenomena using structured illumination

Elias Kristensson,[1,*] Mattias Richter,[1] Sven-Göran Pettersson,[1] Marcus Aldén,[1] and Stefan Andersson-Engels[2]

[1]Division of Combustion Physics, Lund Institute of Technology, Box 118, S-221 00, Lund, Sweden

[2]Division of Atomic Physics, Lund Institute of Technology, Box 118, S-221 00, Lund, Sweden

*Corresponding author: elias@kristennson@forbrf.lth.se

Received 9 April 2008; accepted 16 May 2008;
posted 3 July 2008 (Doc. ID 94780); published 17 July 2008

A method for 3D mapping of scattering particle concentration in a gaseous medium based on the back-scattered light in a single direction has been demonstrated. The technique is originally developed for microscopy but now implemented on larger-scale samples. The technique used is known as *structured illumination*, where a sinusoidal grid pattern is projected onto the medium, thus marking the in-focus plane. This makes it possible to discriminate against light originating from the out-of-focus parts of the sample, which usually makes it difficult to detect inner structures of the medium. In this study a flow of nitrogen was introduced into a flow of water droplets, with the aim to optically select only the plane where nitrogen was present. The results indicate that the technique could be used to study, e.g., combustion devices with limited optical access. © 2008 Optical Society of America

OCIS codes: 110.3010, 280.1350.

1. Introduction

Laser radiation holds many excellent qualities for diagnostic purposes, in particular for studies of gases. This is primarily due to the narrow absorption bands associated with most gases, compared to solids and liquids. Therefore, laser-based studies of gases may be species specific, and by using a pulsed laser system, one can obtain sufficiently high temporal resolution to resolve a turbulent flow. Laser-based approaches may allow temperature, flow fields, and species concentration mapping [1–3], to name a few, to be measured.

Since a laser beam may be focused very sharply into a minuscule volume, micrometer-scale spatial resolution can be obtained. However, many laser-based approaches are not restricted to one dimension, and by instead performing a 2D measurement, additional information is gained. In general, 2D imaging of a semi-transparent medium is relatively easy to perform by the use of laser sheet optics, which simultaneously can also provide good spatial and temporal resolution. Particulary for combustion research, this approach is commonly used, e.g., for cycled-resolved fuel visualization in engines [4] or in gas turbines [5]. However, in order to achieve this, two-way optical access is needed. For engine measurements, a so-called *optical engine* is most commonly used, having a piston of quartz glass and where the walls of the combustion chamber are replaced by a quartz liner. Unfortunately, due to the thermal boundaries of the glass [6], these engines differ from nonoptical ones. Also, due to the damage threshold of glass, higher loads and revolutions per minute (rpm) must be avoided. One solution to minimize the use of glass and still get a 2D visualization, is to use a single-ended (one optical access) approach. This is also true for large industrial combustion applications, such as furnaces and also for characterization of fires, where two-way optical access may not be possible.

0003-6935/08/213927-05$15.00/0

The main reason why 2D imaging with only one optical access is challenging is because of the so-called out-of-focus photons. These photons originate from the parts of the sample that are not within the depth of field of the imaging system, and this creates a blurring effect on the resulting image. One approach to reduce the intensity of this light is to use a so-called *obscuration disk*. Here, the center of the imaging lens is covered in order to discriminate against photons not having a certain incoming angle. Now, only photons originating from within the depth of field of the imaging system will be imaged properly [7]. Unfortunately, this technique is only applicable for point measurements. The reason for this is that in two dimensions, out-of-focus photons that originate from parts of the sample lying off the optical axis may now have the same incoming angle as those originating from the in-focus part of the sample.

A potential single-ended technique, currently under development, is based on an ultrashort pulsed laser system in the picosecond region [8]. Here, the depth resolution is obtained by temporally resolving the backscattered light. The main drawback with this method is the complexity and high cost of the system, since both a picosecond pulsed laser and a camera with adequate time resolution are needed.

In microscopy, where single optical access is a normal approach, another technique, known as *structured illumination*, to discriminate against the out-of-focus light has been developed [9]. With this technique it is possible to separate the light coming from the in-focus plane of the sample from all other detected light, so-called *optical sectioning*. This is made possible by using spatially modulated illumination and is based on the fact that only the zero spatial frequency order is not attenuated by defocusing. Any spatial modulation of the excitation light will therefore only be visible in the in-focus plane of the sample. In this study we investigate the possibility of using structured illumination on a gaseous sample with an inner structure that would be very difficult to observe when allowing all backscattered light to reach the detector.

2. Theory

Structured illumination is a technique commonly used for microscopy to enhance contrast by discriminating against out-of-focus light and is described in detail in [9–11]. The technique is based on spatially modulated illumination, where a grating is projected onto the sample. The main idea is that all nonzero spatial frequencies, i.e., light with an intensity modulation, of the excitation light are heavily attenuated by defocusing, whereas the nonmodulated dc component (the zero spatial frequency) on the other hand is only weakly attenuated with defocus.

A sinusoidal grating yields a fringe pattern $s(x,y)$ of the form

$$s(x,y) = 1 + m \cdot \cos(2\pi\nu x + \phi_0), \tag{1}$$

where m denotes the modulation depth, ν is the spatial frequency, and ϕ_0 is an arbitrary spatial phase, while x and y denote the coordinate axes. The reflected light can be described mathematically as

$$I(x,y) = I_C + I_S \cdot \cos(2\pi\nu x + \phi_0). \tag{2}$$

Here I_C denotes the conventional backscattered image, i.e., the resulting image when all backscattered light is allowed to reach the camera. The optically sectioned image (I_S) contains only light from the in-focus plane of the sample, since, as previously mentioned, it is only in this plane that the grating is efficiently imaged. The cosine term describes the superimposed fringe pattern, which, in order to obtain the true sectioned image I_S, must be removed. This is done by recording three images, I_1, I_2, and I_3, with the relative spatial phases (ϕ_0) 0, $2\pi/3$, and $4\pi/3$, which simply means that the intensity modulation is shifted a third of a period between the images. However, the effect of this shift will be visible only in the in-focus plane, and apart from this, the three images will be identical to each other. By studying the differences among these three images, out-of-focus light, together with the intensity modulation, is removed. It can be shown that

$$I_S = \frac{\sqrt{2}}{3}[(I_1 - I_2)^2 + (I_1 - I_3)^2 + (I_2 - I_3)^2]^{1/2} \tag{3}$$

and that

$$I_C = \frac{I_1 + I_2 + I_3}{3}. \tag{4}$$

Thus, both the conventional and the optically sectioned image can be extracted from the three spatially modulated images. However, great accuracy of the lateral movement of the grid pattern is needed, since incorrect positioning of the pattern can lead to residual spatial modulation being superimposed on the sectioned image [10].

The sectioning strength (depth resolution) depends mainly on two factors, the frequency of the modulation and the depth of field of the imaging system, and can be determined by measuring the modulation depth while moving a reflecting test object through the focus [11].

To further explain the principle of structured illumination a simplified example is shown in Fig. 1, where two of the three spatially modulated images, Figs. 1(a) and 1(b), together with the conventional image, Fig. 1(c), and the optically sectioned image, Fig. 1(d), are shown. To simplify matters, all images are normalized to unity and the intensity modulation is maximized, i.e., $m = 1$, in Eq. (1). The example consists of two layers, one in focus and one positioned either in front of or behind the focus plane. In accordance with previous statements, the modulation of the intensity is visible only in the in-focus plane. The sectioned image is created by implementing

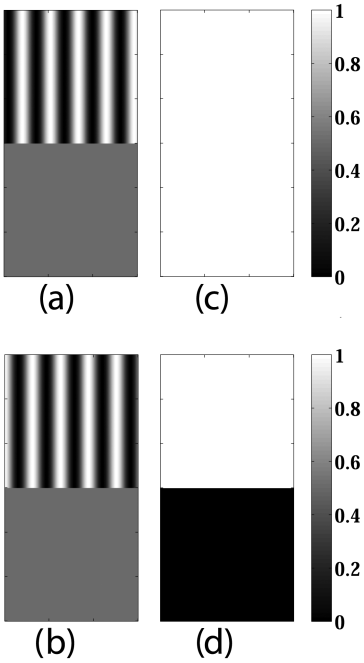

Fig. 1. Example of structured illumination. In (a) and (b) two of the three spatially modulated images, I_1, I_2, and I_3, are shown. The conventional image I_C is shown in (c), and the optically sectioned image I_S is shown in (d). The sample contains two planes, one in focus (upper plane), where the intensity modulation is visible, and one positioned either in front of or behind the focus plane (lower plane). As can be seen in (c), conventional backscattered imaging gives no depth resolution, since the intensity is equally large in both planes. The out-of-focus light is removed by studying the differences between the spatially modulated images, i.e., implementing Eq. (3).

Eq. (3) on the three spatially modulated images, while the conventional image is created by using Eq. (4). As can be seen, the intensity in both planes is equally large, i.e., no depth resolution can be obtained by allowing all backscattered light to reach the camera [Fig. 1(c)]. When discriminating against unmodulated light the intensity in the out-of-focus plane is reduced to zero, showing the true optically sectioned image [Fig. 1(d)].

3. Experimental Setup

A schematic of the experimental setup is shown in Fig. 2. The detection system used in this study consisted of a 12 bit intensified CCD, with 960 × 1280 pixels. The laser was a frequency-doubled Nd:YAG ($\lambda = 532$ nm) running at a repetition rate of 10 Hz. Since the optical sectioning technique gives the best result when using a homogeneous flat laser profile, only the central part of the beam was selected by using three apertures. Also, to remove higher spatial frequencies and thus further improve the beam profile, the beam was sent through a spatial filter. Due to the higher light efficiency of a square ruling (compared to a sinusoidal [10,11]), a Ronchi ruling (5 line pairs/mm) was used. However, the higher spatial frequency orders associated with a square ruling were filtered out with a second spatial filter, since it

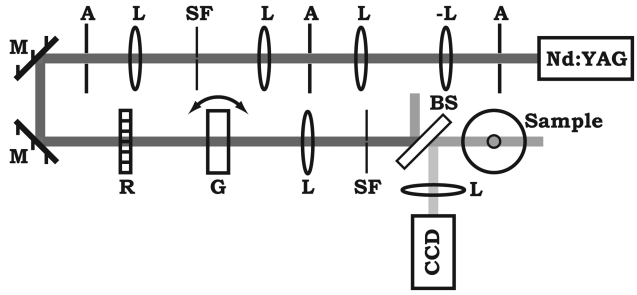

Fig. 2. Schematic of the experimental setup. L = lens, A = aperture, M = mirror, R = Ronchi ruling, SF = spatial filter, G = glass plate, BS = beam splitter.

is only the zero and first frequency order, i.e., a pure sinusoidal fringe pattern, that are to be used in the structured illumination. This was merely a precaution to avoid effects caused by higher order frequencies and is normally not necessary, since higher order frequencies are often attenuated enough by the optical transfer function of the imaging system [11]. Instead of actually moving the grating, the grid pattern was moved a third of a period laterally by tilting a plane-parallel glass plate that was located behind the grating.

In order to establish whether optical sectioning is possible for nonsolid objects, a flow of water droplets was studied, generated by a so-called nebulizer, shown in Fig. 3. In this image the shaded gray area indicates the imaged area, approximately 16× 14 mm^2. In this sample an internal structure, which differs from the water droplets in terms of reflectivity, was introduced. The aim of this was, for demonstrative purposes, to optically select the layer where this internal structure, which in this case was a flow of nitrogen, was visible. The two flows were assumed to be sufficiently stable and separated from each other close to the outlet of the nebulizer, while, due to fluid dynamics, mixing between the flow of water and nitrogen will occur higher up. To confirm this assumption,

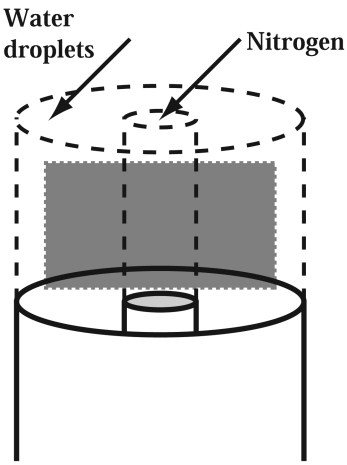

Fig. 3. Close-up of the nebulizer, where the different flows (water droplets and nitrogen) are indicated as dashed cylinders. The approximate area of investigation (16 × 14 mm^2) is indicated with the gray shaded area.

a planar Mie scattering image was recorded (using the two-direction access geometry), where a frequency-doubled Nd:YAG laser, also running at 10 Hz, was used.

4. Results and Discussion

In Figs. 4(a) and 4(d) one of the three spatially modulated images is shown for 1 and 20 accumulations, respectively. Although it should be noted that one accumulation simply means that only one set of three spatially modulated images (I_1, I_2, and I_3) was used, while for 20 accumulations, 20 sets were used. As described above, both the conventional image and the sectioned image are recorded simultaneously, either by summation [Eq. (4)], which gives the conventional image, or by studying the differences between the images I_1, I_2, and I_3 [Eq. (3)], resulting in the optically sectioned image. The resulting conventional images are shown in Figs. 4(b) and 4(e). Here, due to out-of-focus light reaching the detector, the internal structure is extremely smeared out. The out-of-focus light is efficiently removed by the use of structured illumination, shown in Figs. 4(c) and 4(f), with the same number of accumulations as indicated for Figs. 4(a) and 4(d). Here, the internal structure created by the flow of nitrogen is clearly visible in both sectioned images.

The signal strength for one accumulation is enough to view the typical behavior of the two flows. However, since the three images, I_1, I_2, and I_3, were not recorded within the time scale for which movements occur within the flows, this sectioned image will suffer from differences in the flows that have occurred during the time of image recording. This image should therefore rather be seen as a demonstration of the promising possibility to measure on a single-shot basis. When recording 20 accumulations, fluctuations within the two flows are evened out, and Fig. 4(f) shows the possibility to get depth resolution for single-ended measurements on stable flows. In order to remove high frequency spatial noise arising from shot-to-shot variations in the laser, the images are convoluted with a Gaussian filter.

The depth resolution is shown in Fig. 5, where the first order spatial frequency, i.e., the intensity of the modulation, is divided by the zeroth order. The sectioning strength is determined by the full width at half-maximum of the curve, which in this case was found to be, by the use of polynomial curve fitting, approximately 4.0 mm. Increasing the modulation frequency will provide a lower value but decrease the signal-to-noise ratio, since a thinner section will be probed [10] and eventually the signal will be lost in the noise. The sectioning strength could also be increased by decreasing the depth of field of the imaging system. However, to decrease the depth of field a higher magnification is usually needed and by increasing this, the part of the sample that is imaged will decrease. Therefore, the choice of both modulation frequency and depth of field will be dependent on the sample of interest. In this study, the sample dimensions were, for the flow of water droplets ~20 mm and for the inner flow of nitrogen ~5 mm. Since the aim was to study this inner flow, an area of investigation was set to approximately 16 × 14 mm^2 (in order to image a reasonable part of this flow).

As previously mentioned, to investigate whether the flow motions seen in Figs. 4(c) and 4(f) are correct, a planar Mie scattering image was recorded. This image, also consisting of 20 accumulations, is presented in Fig. 6. In this it can be seen that when

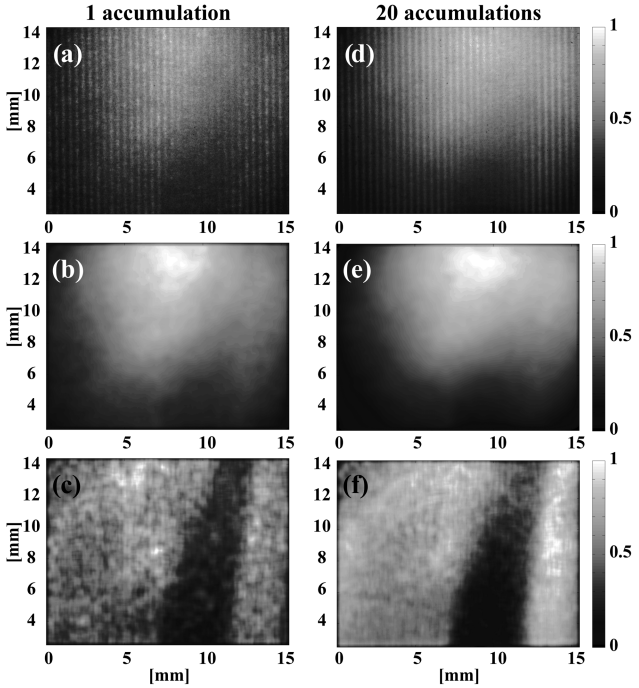

Fig. 4. In (a) and (d) I_1 is shown for 1 and 20 accumulations, respectively, where the superimposed grating pattern can be seen. (b) and (e) Conventional backscattered images for the same number of accumulations. The internal structure created by the flow of nitrogen is extremely smeared out in both of these cases. When the out-of-focus light is removed by means of structured illumination, the internal structure is clearly visible, as shown in (c) and (f).

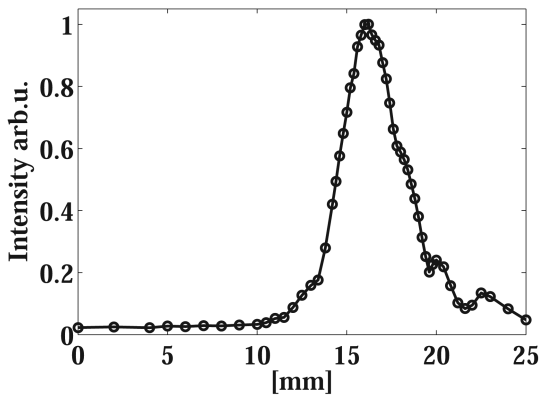

Fig. 5. Determination of the depth resolution of the imaging system. A reflecting test object is moved through the focus, and the modulation depth is measured. This was done by dividing the first order frequency, i.e., the modulation strength, by the zero order frequency, and here it is presented as a function of the position of the test object.

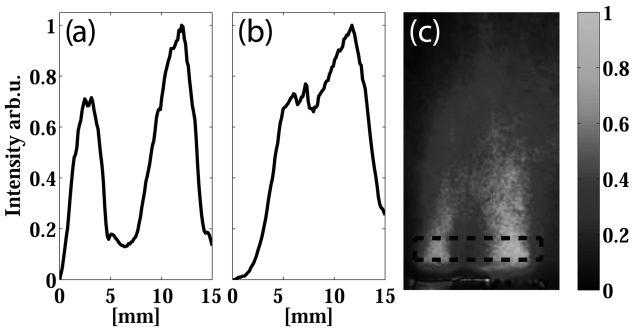

Fig. 6. Planar Mie scattering from the nebulizer. Cross section (a) when the flow is turned on and (b) when it is turned off. The planar Mie scattering image, where the nitrogen is turned on, can be seen in (c), where the dashed lines indicate the heights above the outlet between which the cross section has been calculated.

the flow of nitrogen is turned on, a region that is basically free from water droplets is created, consistent with the optically sectioned images. Also presented in this figure are two cross sections where the nitrogen flow is either on or off. The summation limits for these cross sections are indicated in the figure as dashed lines. The reason why the intensity does not reach zero in Fig. 6(a) is most probably due to multiple scattering events occurring within the flow of water particles.

5. Conclusions

In summation, we have demonstrated the possibility to obtain depth resolution for single-ended measurements on a gaseous medium by using structured illumination. The technique was, in this proof-of-principle, tested on a flow of water droplets and nitrogen based on a Mie scattering measurement. However, structured illumination can further be implemented on other techniques, such as laser-induced fluorescence, thus allowing single species detection. Conventional backscattering Mie imaging and structured illumination have been compared, showing promising results in depth resolution. The technique has further been compared with a 2D laser sheet measurement, with detection at 90°, with qualitative visual agreement.

As described above, the sectioned image is created by studying the differences between the three intensity modulated images. Therefore, one (although more expensive) approach to create a more correct single-shot measurement may be to use three different laser sources. However, since the sectioned image only contains information from the in-focus plane its intensity is much weaker compared to the total detected intensity. This is due to the large contribution of the zero spatial frequency order, which, in order to obtain the sectioned image, is removed. Should these images contain any differences apart from the intensity modulation, such as differences in the laser profiles, this will lead to an incorrect sectioned image, making the use of three different laser sources a more challenging approach.

Another, also more complex solution, in which different laser profiles could be avoided, may be to use a laser with a high repetition rate combined with a high speed imaging system. Such an approach may allow backscattering imaging of, e.g., turbulent flows.

Finally, the authors wish to show their appreciation to the Linné Center within the Lund Laser Center as well as the Centre for Combustion Science and Technology through SSF and STEM for financial support.

References

1. A. C. Eckbreth, *Laser Diagnostics for Combustion Temperature and Species* (Gordon and Breach, 1996).
2. K. Kohse-Höinghaus and J. B. Jefries, *Applied Combustion Diagnostics* (Taylor & Francis, 2002).
3. K. Kohse-Höinghaus, R. S. Barlow, M. Aldén, and J. Wolfrum, "Combustion at the focus: laser diagnostics and control," in *Proceedings of the Combustion Institue* (Elsevier, 2005), pp. 89–123.
4. J. Olofsson, H. Seyfried, M. Richter, M. Aldén, A. Vressner, A. Hultqvist, B. Johansson, and K. Lombaert, "High-speed LIF imaging for cycle-resolved formaldehyde visualization in HCCI combustion," SAE 2005-01-0641 (2005).
5. R. Sadanandan, M. Stöhr, and W. Meier, "Simultaneous OH-PLIF and PIV measurements in a gas turbine model combustor," Appl. Phys. B **90**, 609–618 (2008).
6. S. T. Sanders, T. Kim, and J. B. Ghandhi, "Gas temperature measurements during ignition in an HCCI engine," SAE2003-01-0744 (2003).
7. A. C. Eckbreth and J. W. Davis, "Spatial resolution enhancement in coaxial light scattering geometries," Appl. Opt. **16**, 804–806 (1977).
8. B. Kaldvee, A. Ehn, J. Bood, and M. Aldén, "Development of a Picosecond-LIDAR System for Combustion Diagnostics," in *Laser Applications to Chemical, Security and Environmental Analysis*, OSA Technical Digest (CD) (Optical Society of America, 2008), paper LWC5.
9. M. A. A. Neil, R. Juskatitis, and T. Wilson, "Method of obtaining optical sectioning by using structured light in a conventional microscope," Opt. Lett. **22**, 1905–1907 (1997).
10. M. J. Cole, J. Siegel, S. E. D. Webb, R. Jones, K. Dowling, M. J. Dayel, D. Parsons-Karavassilis, P. M. W. French, M. J. Lever, L. O. D. Sucharov, M. A. A. Neil, R. Juškaitis, and T. Wilson, "Time-domain whole-field fluorescence lifetime imaging with optical sectioning," J. Microsc. **203**, 246–257 (2001).
11. S. E. D. Webb, Y. Gu, S. Lévêque-Fort, J. Siegel, M. J. Cole, K. Dowling, R. Jones, P. M. W. French, M. A. A. Neil, R. Juškaitis, L. O. D. Sucharov, T. Wilson, and M. J. Lever, "A wide-field time-domain fluorescence lifetime imaging microscope with optical sectioning," Rev. Sci. Instrum. **73**, 1898–1907 (2002).